

## MICROSTRUCTURAL VARIATIONS OF SMOKES FROM ANALYSIS OF DIAGRAMS OF LIGHT-SCATTERING PARAMETERS

R.F. Rakhimov and V.S. Kozlov

*Institute of Atmospheric Optics,  
Siberian Branch of the Russian Academy of Sciences, Tomsk  
Received January 16, 1998*

*The dynamics of microstructural variations in smokes of pyrolysis origin at their relaxation in a closed volume is considered by comparing the diagrams of polarization measurements of aerosol scattering parameters with the model estimates. From the analysis of experimental data, peculiarities in transformation of the disperse composition of pyrolysis smokes were noticed in different ranges of the size spectrum. It is found that smoke particle number density at smoke generation is a scaling factor in formation of smoke optical and microphysical characteristics. The dynamics of parameters of the microdisperse fraction follows the typical coagulation variation of a spectrum with the shift of the modal radius from  $r_{1m}^{(3)} = 0.042 \mu\text{m}$  at the initial stage of measurements to  $r_{1m}^{(3)} = 0.075 \mu\text{m}$  (particle enlargement) in two hours. At the same time, the coarse-disperse fraction is characterized by significant decrease in both the particle number density and the volume concentration while the modal radius  $r_{3m}^{(3)}$  shifts insignificantly from 1.09 to 0.869  $\mu\text{m}$  and the distribution mode relatively narrows. The latter may be caused by an increase in compactness of the morphological structure of large smoke particles. The process of large particles sedimentation upon the chamber walls prevails over the processes of coagulation enlargement, thus causing the marked decrease in the particle number density in this range of the particle size spectrum.*

### INTRODUCTION

In response to effect of various atmospheric processes, several microphysical characteristics of the state of an aerosol component change simultaneously, as a rule. The range of their change is sometimes so wide that the use of only one parametrical dependence for the analysis of the mechanism of this response is insufficient in many cases. In this connection, solution of the inverse problem for identification of microstructural variations of the aerosol phase under the conditions when both the particle size spectrum and the optical constants of particle matter are simultaneously subject to change becomes very complicated. Moreover, in passing from one size range to another, a definite specificity is observed in formation of the morphology and the chemical composition of particles, i.e., the refractive index may vary with different rate for subfractions within a given size spectrum. Therefore, for investigation into the real mechanism of action of one or another factor on the process of formation of an aerosol component in the atmosphere, combined optical measurements are required. Such measurements should be chosen in such a way to contain maximum information on the indicated complex of microstructural variations.

About the same situation takes place when studying aerosols generated from thermal decomposition of wood and other combustibles, i.e. the processes generating so-called smoke aerosols. According to Newberg estimates,<sup>1</sup> about  $10^{22}$ – $10^{23}$  small particles come to the atmosphere during medium-size forest fire from an area of one hectare. On moderation of exchange processes in the low tropospheric layer, heavy forest fires can provoke an appearance of local anomalous accumulation of aerosols with relatively high concentration of the fine-disperse fraction. The "smoke haze" observed over vast expanses of West Siberia in October, 1997, may serve as a prominent illustration to such anomalous enhancement of the atmospheric turbidity.<sup>2</sup>

Estimating the possibilities of the most popular methods for interpretation of optical measurement based on solution of the inverse problem of aerosol scattering, we can hope to only an approximate solution which allows optimization of the data of optical measurements over an obviously simplified class of aerosol microstructure models. So, for example, the model conception ignoring the physical and chemical variability of fractions, their morphological variety, and the independent dynamics of the size spectrum and the optical constants of particles from different aerosol

fractions, is obviously inconsistent for identification of microstructural changes in smoke aerosols, because it noticeably distorts the real pattern of physical processes in a smoke.

We have approved a somewhat different approach to the study of the formation dynamics of the smoke aerosol microstructure. Earlier, in Refs. 3 and 4, the quantitative estimates of the variability range of some microstructural characteristics of pyrolysis smokes were obtained in the approximation of the unimodal form of the aerosol particle size distribution based on the analysis of optical diagrams of the interrelated dynamics of aerosol scattering parameters.

Here the method of the diagram analysis is used for more complicated theoretical estimates, and so it received further development effort. The used theoretical estimates are based on the method fraction-by-fraction reduced determination of the formation dynamics of the smoke aerosol size spectrum. Changes in the smoke microstructure were analyzed based on a comparison of the diagrams of interrelated variation of the scattering parameters, obtained from the results of polarization nephelometry of pyrolysis aerosols, with the similar data computed for the case of multicomponent polydisperse mixture. Therewith both the variation of individual parameters of the size spectrum in an isolated fraction and the dynamics of integral characteristics of the disperse structure elements were under control when modeling the theoretical data.

## EXPERIMENT

The results of polarization measurements of the scattering phase functions of wood smokes were used as the initial experimental information. These functions were obtained under the controllable conditions with a polarization nephelometer at  $\lambda = 0.63 \mu\text{m}$  wavelength.<sup>3</sup> The smoke aerosol was generated by the pyrolysis method, i.e., from putrefaction of the wooden specimen in a heating element at  $T \sim 400\text{--}500^\circ\text{C}$  without flame. Such low-temperature decomposition of the wooden specimen resulted in filling the aerosol chamber of  $0.1 \text{ m}^3$  volume with smoke particles. The process of formation of the smoke aerosols and evolution of their microstructure was investigated in the chamber at the relative air humidity of 30–40% and the temperature  $\sim 20^\circ\text{C}$ . During the experiment, the normally polarized components of the scattering phase function  $g_1(\theta)$  and  $g_2(\theta)$  were sequentially measured with the nephelometer (within the range of scattering angles  $\theta = 5\text{--}170^\circ$ ) with an average relative error of 5–10%. One measurement act of the polarization phase function lasted about 3 min.

The angular dependence of the phase function of non-polarized radiation (the coefficient of directed scattering)  $g(\theta) = (g_1(\theta) + g_2(\theta))/2$ , as well as the degree of linear polarization of the scattered light  $p(\theta) = (g_1(\theta) - g_2(\theta))/(g_1(\theta) + g_2(\theta))$  were

calculated from the measured polarization components of the phase function.

In order to analyze microstructural changes in pyrolysis smokes, the diagrams of interrelated dynamics of the following parameters of the aerosol scattering were studied (in various combinations of pairs):

- the asymmetry coefficient  $K_a$  of the phase function  $g(\theta)$  equal to the ratio of the scattered radiation fluxes into front and back hemispheres;
- the polarization degree at angles  $\theta = 110^\circ$  and  $165^\circ$  designated as  $P_1$  and  $P_2$ , respectively;
- the ratios  $A_s = g(15^\circ)/g(110^\circ)$  and  $D_s = g(165^\circ)/g(110^\circ)$  characterizing the degree of elongation of the phase function in the forward and backward directions.

The choice of these parameters is caused by both numerous theoretical estimates<sup>4–6</sup> for aerosol formations of the type of atmospheric haze and the content of the single-parameter model<sup>7,8</sup> determined empirically. As follows from them, the parameters  $A_s$  and  $D_s$  are in essence the ratio of the phase function values indicating the maximum dynamics of oscillations under variation of the atmospheric turbidity. At the same time, they have a higher sensitivity to variations of the parameters of the disperse structure elements and the optical constants of particles of different fractions.

Values of the polarization degree at the angle  $\theta = 100^\circ$  are rather sensitive to changes of the size spectrum of both the microdisperse and accumulative fractions (the distribution mode width and the modal radius), as well as to the interrelated dynamics of integral characteristics of their microstructure. The values of  $P_2$  and  $K_a$  (the asymmetry coefficient of the scattering phase function) are sensitive to the size distribution and the refractive index of the haze of the middle- and coarse-disperse fractions, whereas parameter  $D_s$  strongly depends on a choice of a model value of the complex refractive index (CRI) of particles, particularly, to its imaginary part (“sloping” type of the phase function for strongly absorbing particles<sup>3,5,6</sup>). Thus selected parameters in various pair combinations allow us, as further model estimates show, to follow the sufficiently fine changes in microphysical structure of smoke aerosols.

## RESULTS

For analysis we have used only six types of diagrams (Figs. 1–3) generalizing about 500 experimentally obtained angular dependences of the phase function and the degree of polarization.<sup>3</sup> The preliminary analysis of the experimental data allows us to conclude that the phase function is characterized by significant variability of its forward and backward elongation parameters. The angular dependence of the polarization degree varies in its shape from the curves with the positive polarization maximum at  $\theta = 100^\circ$  to appearance of two extrema or one deep maximum of negative polarization at  $\theta = 150\text{--}160^\circ$ . A comparison of the smokes optical

characteristics with the computed data for some main types of the atmospheric aerosol has shown a significant similarity between the smokes and the atmospheric hazes in shape peculiarities and the variability range (Fig. 4).

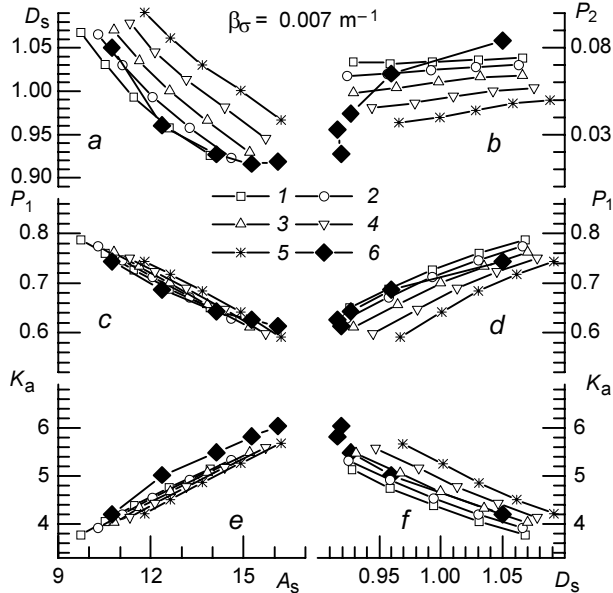


FIG. 1. Diagrams of interrelated variation of the scattering parameters: the calculated data at different values of the microstructural parameters (1-5); the results of polarization measurements for the smoke particle number density in the chamber  $\beta_{\sigma} = 0.007 \text{ m}^{-1}$  (6).

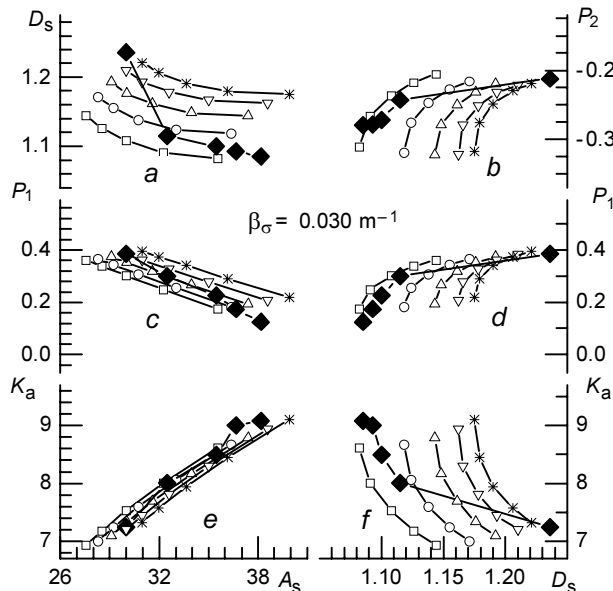


FIG. 2. Diagrams of interrelated variation of the scattering parameters: the calculated data (1-5); the results of polarization measurements for the smoke particle number density in the chamber  $\beta_{\sigma} = 0.030 \text{ m}^{-1}$  (6).

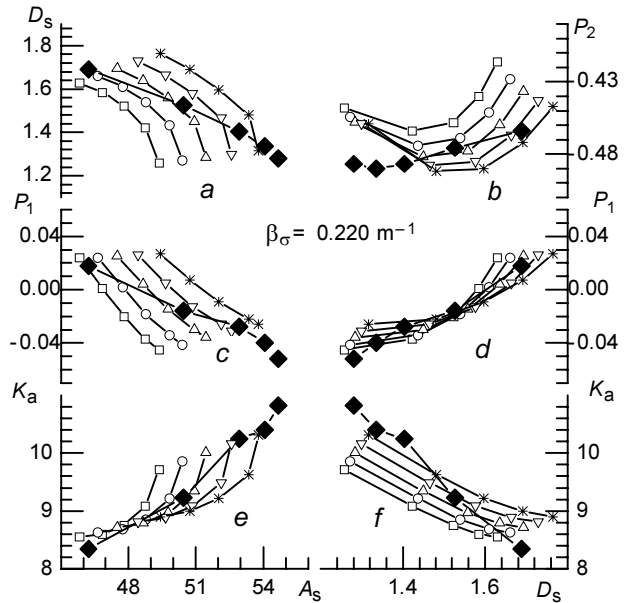


FIG. 3. Diagrams of interrelated variation of the scattering parameters: the calculated data (1-5); the results of polarization measurements for the smoke particle number density in the chamber  $\beta_{\sigma} = 0.220 \text{ m}^{-1}$  (6).

In the diagram analysis of the experimental data, the numerical estimates of the aerosol scattering parameters were used, which were obtained based on the three-fraction model of the size spectrum<sup>5</sup>:

$$f(r) = \frac{dN}{dr} = \frac{v(r)}{4\pi r^3} = A^{(v)} r^{-v} \times \sum_{i=1}^k M_i^{(v)} \exp \{-b_i [\ln(r/r_i^{(v)})]^2\}. \quad (1)$$

When drawing the calculated diagrams, the shape parameters of the scattering phase function and the polarization degree were estimated using an independent set of CRI values for each fraction. Thus, we have used six input parameters of the refractive index in addition to the nine parameters of the size spectrum given by Eq. (1). In order to reduce the number of possible versions of model estimates, we have succeeded in implementation of the unidirectionality principle for changes of the microstructural parameters of an isolated fraction.

For the fine-disperse fraction ( $i = 1$ ) the process of coagulation transformation of the disperse structure was considered (as a hypothesis) as an origin of coordinated dynamics of variation of the modal radius and the distribution mode width.

The dynamics of the above-mentioned parameters of the size spectrum of the given fraction practically coincided with that determined earlier based on the specially developed method of reduced modeling of the coagulation transformation of the spectrum,<sup>9</sup> i.e.,

using the system of differential equations for integral characteristics of the size spectrum of the given fraction

$$\frac{dN_i}{dt} = -\frac{K}{2} N_i^2 - \beta N_i + \gamma N_j, \quad (2)$$

$$\frac{dL_i}{dt} = -\beta L_i + \gamma L_j, \quad (3)$$

$$\frac{dW_i}{dt} = -\frac{K}{\pi} L_i^2 - \beta W_i + \gamma W_j, \quad (4)$$

where  $L_i$  and  $W_i$  are the second and the third moments of the size spectrum for particles of the given distribution mode;  $K$ ,  $\beta$ ,  $\gamma$  are the "rown coagulation constant and the coefficients determining the efficiency of particle sink to the chamber walls and replenishment of the given range of particles due to their transition from the neighbor one.

This analysis was performed based on the results of polarization measurements obtained at the second stage of smoke evolution, the so-called "aging" stage, when direct action of the source of pyrolysis generation had already resulted in complete decomposition of the wooden specimen under study. Therefore, the coefficient  $\gamma$  was in fact set zero. In this case, the solution of the system of equations (2)–(4) determined the behavior of the disperse system in the absence of source:

$$N_i(t) = 2\beta N_{i0} / [(KN_{i0} + 2\beta) \times \exp(2\beta t) - KN_{i0}], \quad (5)$$

$$L_i = L_{i0} \exp(-\beta t), \quad (6)$$

$$W_i(t) = \left\{ W_{i0} - \frac{KL_{i0}^2}{\pi\beta} [\exp(-\beta t) - 1] \right\} \exp(-\beta t). \quad (7)$$

Having known the variability dynamics of the integral characteristics of the size spectrum for the fine-disperse fraction, it is easy to estimate the dynamics of the modal radius and the width of the distribution mode.

The modeling method approved in Refs. 5 and 6, as well as the obtained results has shown that modeling of the coagulation transformation under the assumption of close volume packing of coagulating particles well corresponds to the dynamics of microstructural parameters for the fine-disperse fraction and differs to some extent from the dynamics of real processes regulating the disperse composition of the second and third fractions.

The process of particle sink to the chamber walls for the coarse-disperse fraction ( $i = 3$ ) was considered as the basic factor in modeling its transformation dynamics. The further estimates have shown that active sink of smoke particles to the chamber walls was characteristic of the medium-disperse fraction ( $i = 2$ ) as well.

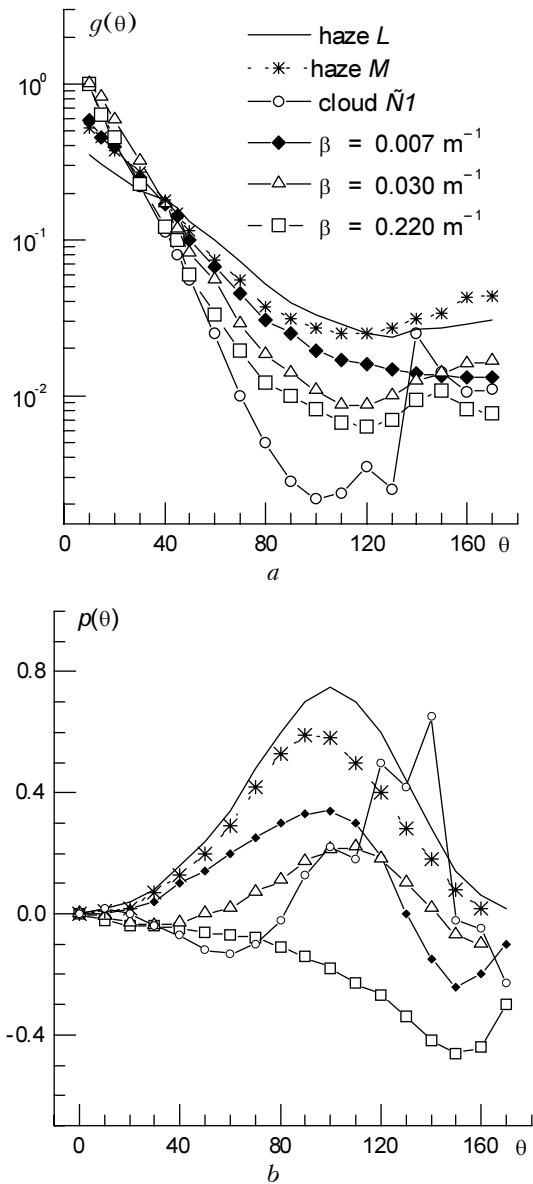


FIG. 4. Variation of the shape of the scattering phase function (a) and the angular dependence of the polarization degree vs. the smoke particle number density in the chamber:  $\beta_{\sigma} = 0.007, 0.030, 0.220 \text{ m}^{-1}$  in comparison with the calculated data for aerosol hazes M and L and for a cloud C1.

The polarization measurements allowed us to study transformation peculiarities of the optical-microstructural characteristics at "aging" of the smoke aerosol as a function of the smoke particle number density in the air. As the mass of a burned material increased from 3 to 20 mg, the scattering coefficient  $\beta_{\sigma}$  changed from 0.006 to 0.3  $\text{m}^{-1}$ . The smoke particle number density was found to be an important scaling factor in formation of the smoke optical-microphysical parameters. The most stable regularity of the "aging" process of the pyrolysis smoke is an increase of the

asymmetry coefficient of the phase function and its forward peak at simultaneous lowering of the scattering efficiency in the backward direction.

As a result of numerous simulations, we managed to find the vicinity of mutually consistent dynamics of microstructural and optical characteristics and to obtain their acceptable correspondence to the results of

polarization measurements (see Figs. 1–3). At the same time, we have found the variability range of the refractive index of all the three fractions (the real part within the range from 1.690 to 1.520 and the imaginary part within the range from  $-0.12$  to  $-0.004$ ) and the variation dynamics of their size spectrum (Fig. 5) as well.

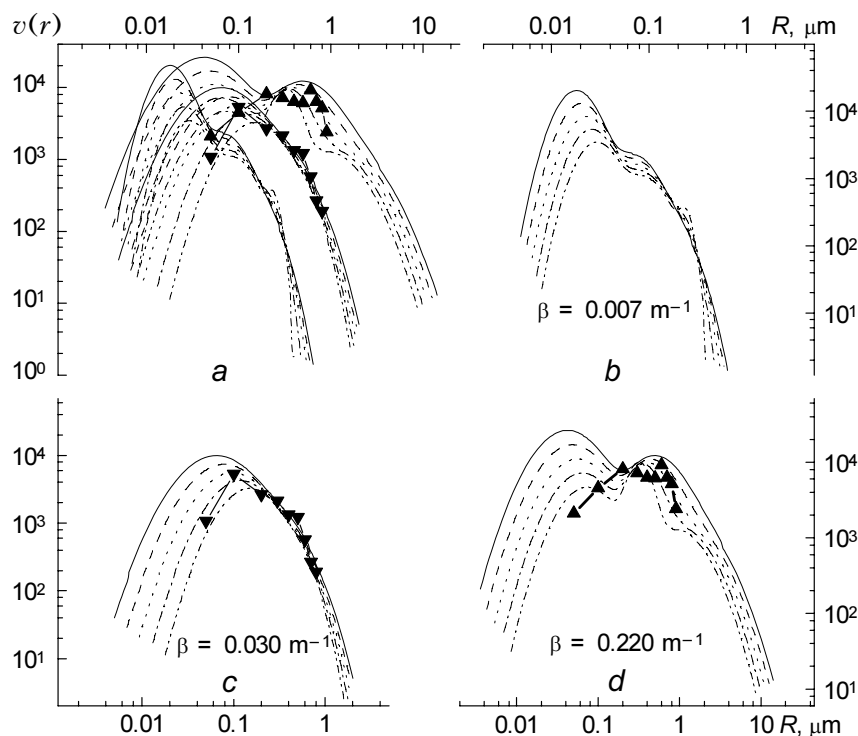


FIG. 5. Variation dynamics of the size spectrum for smoke aerosols at different values of the smoke particle number density in the chamber: *a* comparison of the three cases (*a*);  $\beta_{\sigma} = 0.007 \text{ m}^{-1}$  (*b*),  $\beta_{\sigma} = 0.030 \text{ m}^{-1}$  (*c*),  $\beta_{\sigma} = 0.220 \text{ m}^{-1}$  (*d*); the values of the scattering phase function are given in comparison with the data ( $\tau$ ,  $\sigma$ ) from Ref. 10).

The analysis of calculated data has shown an ambiguity of the evolution dynamics of the size spectrum for different fractions. It proved to depend essentially on the mass of the wooden specimen used in the pyrolysis decomposition.

The calculations have revealed that the modal radius  $r_{1m}^{(3)}$  of microdisperse particles grows in the process of “aging” from  $0.042$  to  $0.075 \mu\text{m}$ . The dynamics of particle size distribution for the coarse-disperse fraction is, in its turn, characterized by significant lowering of both the particle number density and the volume concentration at a small shift of the modal radius  $r_{3m}^{(3)}$  from  $1.09$  to  $0.869 \mu\text{m}$  and relative narrowing of the distribution mode. The latter may be connected with the increased compactness of the morphological structure of large smoke particles.

The size spectrum of the medium-disperse fraction has the similar dynamics. In particular, as the concentration of initial particles decreases significantly (Fig. 5*b–d*), the modal radius  $r_{2m}^{(3)}$

decreases from  $0.488$  to  $0.320 \mu\text{m}$ . Besides, even stronger narrowing of the spectrum is observed, resulting in formation of the sufficiently narrow distribution mode of the medium-disperse fraction (Fig. 5*d*). The process of the particle sedimentation on the chamber walls dominates in this case over the processes of coagulation increase in concentration of coarse particles. Therefore, the distribution mode within this spectral range progressively narrows with time in all the three considered cases (Fig. 5).

It should be noted that the optical constants of pyrolysis particles, which varied in the process of the smoke “aging” from  $m_w \sim 1.69 - i \cdot 0.2$  at the beginning of the measurement cycle to  $1.52 - i \cdot 0.002$  at the end, significantly differ from the similar data for soot ( $m_s \sim 1.87 - i \cdot 0.79$ ) in both the real and imaginary parts of the refractive index. According to the obtained estimates, at low wood amount the specimen subject to pyrolysis decomposition is small ( $\beta_{\sigma} = 0.007 \text{ m}^{-1}$ ), the variability range of the refractive index shifts toward

the values of  $m_s$ , i.e. from  $m_w \sim 1.69 - i \cdot 0.2$  to  $m_w \sim 1.59 - i \cdot 0.04$ . In the second case at  $\beta_\sigma = 0.03 \text{ m}^{-1}$ , the difference is more noticeable: from  $m_w \sim 1.57 - i \cdot 0.01$  to  $m_w \sim 1.52 - i \cdot 0.002$ . In the third case, at  $\beta_\sigma = 0.22 \text{ m}^{-1}$ , the estimates by the diagram method give the intermediate values: approximately from  $1.59 - i \cdot 0.02$  to  $1.57 - i \cdot 0.002$  with relatively weak time dynamics.

### CONCLUSION

Although the developed approach is not rigorous enough for unambiguous interpretation of the obtained results, it allows us to estimate the real complexity of the kinetics of nonequilibrium microprocesses in smokes and to determine a number of problems to be solved for further analysis and *a priori* diagnostics of optical and microphysical properties of smoke aerosols.

The advantage of the proposed approach is that it allows us to analyze the process for several hypotheses of the mechanism of coagulative joining of aerosol particles into one particle. This is of great importance, because, as the obtained results show, the problem of compactness of the morphological structure of coagulants is really urgent. The hypotheses of invariance of the total volume and the integral linear size of a disperse system are the limited cases among a number of packing versions. Though the latter version may seem improbable at first glance because it assumes a growth of the integral volume of the aerosol phase, it cannot be ignored since aerosols in the real atmosphere are constantly surrounded by water vapor, the mass content of which exceeds the aerosol phase by several orders of magnitude. Formation of microcapillaries at mutual adherence necessarily stimulates the process of heterogeneous micropore condensation of moisture, thus ensuring an increase in mass of the aerosol component as well. The problem of further development of the morphology of coagulants and their progressive compacting from friable aggregates into dense formations

is equally important for investigation. The dynamics of the spectrum parameters of the medium- and coarse-disperse fractions (Fig. 5d) is indicative of such a process, what on our opinion is worthy of particular attention and valid for further investigation.

The found difference in the variation dynamics of the optical constants of aerosol particles of the first and second generation is likely to be due to not only an ambiguity of their hygroscopic properties, but the morphologic specificity of fractions interaction with the moisture field as well.

### REFERENCES

1. S. Rasul, ed., *Chemistry of Low Atmosphere* [Russian translations] (Mir, Moscow, 1976), 408 pp.
2. Yu.A. Pkhalagov, V.N. Uzhegov, and N.N. Shchelkanov, in: *Abstracts of Reports at Fourth Workshop on Siberian Aerosols*, Tomsk (1997), pp. 40–41.
3. V.S. Kozlov, "Experimental Investigation of Optical-Microphysical Properties of Smoke Aerosols," Cand. Phys.-Math. Sci. Dissert. Tomsk, (1985).
4. V.S. Kozlov and V.Ya. Fadeev, in: *Proceedings of the Second All-Union Symposium on Atmospheric Optics* (Tomsk, 1980), P. 1, pp. 38–41
5. G.M. Krekov and R.F. Rakhimov, *Optical Models of the Atmospheric Aerosol (TA S" AS USSR*, Tomsk, 1986), 295 pp.
6. G.M. Krekov and R.F. Rakhimov, *Optical Ranging Model of the Continental Aerosol* (Nauka, Novosibirsk, 1982), 200 pp.
7. M.V. Kabanov, M.V. Panchenko, Yu.A. Pkhalagov, et al., *Optical Properties of Coastal Atmospheric Hazes* (Nauka, Novosibirsk, 1988), 202 pp.
8. G.M. Krekov, M.V. Panchenko, and R.F. Rakhimov, in: *Proceedings of the Seventh All-Union Symposium on Laser and Acoustic Sounding of the Atmosphere* (Tomsk, 1982), P. 1, pp. 127–130.
9. R.F. Rakhimov, *Atm. Opt.* **2**, No. 3, 206–212 (1989).
10. V.V. Veretennikov, I.E. Naats, V.S. Kozlov, and V.Ya. Fadeev, *Izv. Akad. Nauk SSSR, Fiz. Atmos. Okeana* **16**, No. 3, 270–276 (1980).